Available online at www.sciencedirect.com
ScienceDirect
Catalysis Today 122 (2007) 277–283
CATALYSIS TODAY
www.elsevier.com/locate/cattod

# Aerobic oxidation of alcohols catalyzed by gold nano-particles confined in the walls of mesoporous silica

Juncheng Hu, Lifang Chen, Kake Zhu, Andreas Suchopar, Ryan Richards *

*School of Engineering and Science, International University Bremen, Campus Ring 8, 28759 Bremen, Germany*

Available online 19 January 2007

**Abstract**

Gold nano-particles confined in the walls of mesoporous silica (GMS) catalysts were successfully prepared by a novel and simple technique utilizing thioether functional groups in the walls of mesoporous silica to anchor $HAuCl_4$. Calcination of the materials removed organic moieties and reduced the gold salt to gold nano-particles. In this procedure, the thioether groups were introduced into the silica wall via a co-condensation of tetraethyl orthosilicate (TEOS) with 1,4-bis(triethoxysily)propane tetrasulfide. These gold containing mesoporous catalysts have unusually high surface area and pore volume. The catalysts were evaluated for the solvent free liquid phase oxidation of benzyl alcohol by molecular oxygen. High selectivity to benzaldehyde was obtained under the reaction conditions of 403 K, 15 atm and 5 h in an autoclave. The 1.5% GMS catalyst was also evaluated for oxidation of alcohols using toluene as solvent under flowing oxygen at atmospheric pressure at 353 K in a two-necked flask. Under these conditions the conversion of benzyl alcohol reached 100% after 2 h and it was demonstrated that the catalyst can be recycled three times without significant loss of activity.


*Keywords:* Gold; Mesoporous silica; Nano-particle; Oxidation; Alcohol

## 1. Introduction

The oxidation of alcohols into the corresponding aldehydes or ketones is one of the most important functional group transformations in organic synthesis [1–3]. The synthesis of aldehydes or ketones by traditional methods using stoichiometric reagents are decreasing, but are still widespread [4]. The development of effective catalytic routes to aerobic oxidation of alcohols using environmentally benign and inexpensive oxidants such as oxygen or air is an important challenge. Recently, the use of molecular oxygen as a terminal oxidant has received great attention for both economic and environmental benefits, and many highly efficient systems have been developed for catalytic aerobic alcohol oxidation using copper, palladium and ruthenium catalysts [5–7]. In recent years, the unexpectedly high activity of gold as a low-temperature CO oxidation catalyst has initiated intensive research in the use of gold nano-particles for the liquid-phase oxidation of alcohols [8,9]. The gold-based catalysts have demonstrated very interesting and promising activity, and different types of gold-based homogeneous and heterogeneous catalysts in the form of metal complex or nano-particles have been developed for the oxidation of alcohols [10–14]. Generally, the catalytic properties of heterogeneous gold catalysts strongly depend on the particle size. The use of gold as a catalyst requires careful and unconventional preparation of the gold particle morphology focusing on achieving a very small gold particle size. One of the key problematic issues that has hampered the applications of gold catalysts is the stability of the particles against sintering under reaction conditions [15]. Recently, in order to obtain highly active gold catalysts, a chemical grafting and reduction process was reported in which amino, thiol or di-amino groups were grafted onto to the surfaces of mesoporous silica, then $HAuCl_4$ was introduced via a neutralization reaction, followed by a reduction procedure [16–18]. This process has proven to be effective to some degree, but the gold nano-particles dispersed on the silica surface (in the channels or outside of the channels) are still problematic since gold is mobile on the surface of silica, it will be easy to sinter under rigid reaction conditions. Here, we present a novel method to synthesize a catalytic system in which the gold nano-particles are highly dispersed and confined in the walls of mesoporous

* Corresponding author. Tel.: +49 421 200 3236; fax: +49 421 200 3229.
*E-mail address:* r.richards@iu-bremen.de (R. Richards).

0920-5861/$ – see front matter © 2007 Elsevier B.V. All rights reserved.
doi:10.1016/j.cattod.2007.01.012

silica, not in the channels. Thus, the channels will not be blocked and the gold nano-particles may not sinter under calcination or reaction conditions. These catalysts provided excellent catalytic performance in the oxidation of alcohols.

## 2. Experimental

### 2.1. Catalysts preparation

Gold nano-particles confined in the walls of mesoporous silica (GMS) were synthesized by dissolving 20 g of Pluronic P123 ($EO_{20}PO_{70}EO_{20}$, $M_{av}$ = 5800, Aldrich) in 750 ml of a 2 M HCl solution, subsequently, a mixture of 41.6 g tetreaethyl orthosilicate (TEOS) and 4.2 g 1,4-bis(triethoxysilyl)propane tetrasulfide were quickly added with vigorous magnetic stirring followed by the dropwise addition of the pre-designated amounts of aqueous $HAuCl_4$ solution. The solution was stirred for 24 h at 313 K and then aged for 72 h at 373 K. The solid was filtered off, washed with water three times and with ethanol twice, dried at 373 K for 24 h and calcined at 773 K for 5 h. According to the different weight percent of gold in the catalysts, these catalysts were called 0.5% GMS, 1.0% GMS, 1.5% GMS, 2.0% GMS, 2.5% GMS and 10% GMS, respectively.

### 2.2. Catalyst characterization

#### 2.2.1. $N_2$ adsorption–desorption isotherms

$N_2$ adsorption–desorption isotherms of the samples were measured at liquid nitrogen temperature with a NOVA 4000e instrument supplied by Quantachrome, Germany. Prior to measurement, the samples were degassed at 523 K under vacuum for more than 4 h. The specific surface areas were evaluated with the Brunauer–Emmett–Teller (BET) method in the $P/P_0$ range of 0.05–0.35. Pore size distribution curves were calculated from the adsorption branch of the isotherms with the Barrett–Joyner–Halenda (BJH) method, and pore sizes were obtained from the peak positions of the distribution curves.

#### 2.2.2. Powder X-ray diffraction

The catalysts were characterized by powder X-ray diffraction (XRD) using a Siemens D5000 X-ray diffractometer with nickel filtered Cu Kα radiation (λ = 1.5418 Å) at a scanning rate of 0.1° $min^{-1}$ in the 2$\theta$ range of 10–80°.

#### 2.2.3. Thermogravimetric analysis

Thermogravimetric analysis was performed using a SDT Q600 instrument supplied by TA Instruments. The samples were placed in an alumina sample holder and heated at a rate of 10 K $min^{-1}$ from room temperature to 1173 K under a $N_2$ flow with a rate of 100 ml $min^{-1}$.

#### 2.2.4. Fourier-transform infrared spectroscopy

For FTIR investigation of the catalyst, a Nicolet 4700 spectrometer with a liquid nitrogen cooled detector and DRIFT accessory was used with the following parameters: 3000 scans, 600–4000 $cm^{-1}$ scan range, 4 $cm^{-1}$ resolution.

A homemade flow cell was used for the in situ measurements. Prior to the experiment, the catalyst was pretreated with flowing nitrogen at 523 K for 2 h to remove any water or other impurities from its surface. A spectrum of the clean catalyst surface was collected following this procedure at the adsorption temperature (353 K) and was used as the background. Adsorption studies were conducted by exposing the catalyst to a stream of flowing nitrogen carrying a small concentration of benzyl alcohol (obtained through passage of the nitrogen stream through a saturator) then exposed to the air flow for 30 min, cooled to room temperature and purged with nitrogen for 30 min to remove gas phase benzyl alcohol and benzaldehyde.

### 2.3. Catalytic tests

For solvent-free oxidation of benzyl alcohol, 3.0 g benzyl alcohol and 50 mg catalyst were placed into a 30 ml autoclave and 15 atm oxygen was charged into the autoclave. It was then heated to 403 K and kept for 5 h at the temperature with a stirring speed of 1000 rpm. After reaction, the catalyst was removed from the reaction mixture by filtration, the products and the unconverted reactants were analyzed by gas chromatography with a flame ionization detector, using a HP-5 column and nitrogen as carrier gas.

For atmospheric pressure oxidation of alcohols under oxygen flow, catalytic experiments were carried out at 353 K, in a two-necked batch reactor fitted with a reflux condenser, oil bath, thermocouple and magnetic stirrer. A mixture of $K_2CO_3$ (10 mmol) and 0.18 g 1.5% GMS in toluene (20 ml) was prepared in a two-necked flask. The flask was then filled with pure oxygen and heated to 353 K. The 10 mmol of alcohol was then added into the solution and the resulting mixture was stirred at 353 K with a stirring speed of 1000 rpm. After reaction, the catalyst was removed from the reaction mixture by filtration, the products and the unconverted reactants were analyzed by gas chromatography with a flame ionization detector, using a HP-5 column and nitrogen as carrier gas.

## 3. Results and discussion

### 3.1. Synthesis and characterization of GMS catalysts

The synthetic method utilized thioether group functionalization of the mesoporous silica walls to introduce $HAuCl_4$ into the framework as shown in Scheme 1. Thus, tetraethyl orthosilicate (TEOS) and 1,4-bis(triethoxysilyl)propane tetrasulfide co-condense forming the thioether group in the framework and effectively anchoring $HAuCl_4$. After $HAuCl_4$ was introduced the material was calcined to reduce the gold and remove the organic moieties yielding the highly dispersed and clear mesoporous silica supported gold nano-particles.

The assembly process was investigated by diffuse reflectance infra-red Fourier transform (DRIFT) spectroscopy. The strong IR adsorption bands at 2883, 2934 and 2970 $cm^{-1}$ in the range of 2800–3000 $cm^{-1}$ in Fig. 1a were assigned to the C–H bonds in the surfactant and 1,4-bis(triethoxysily)propane

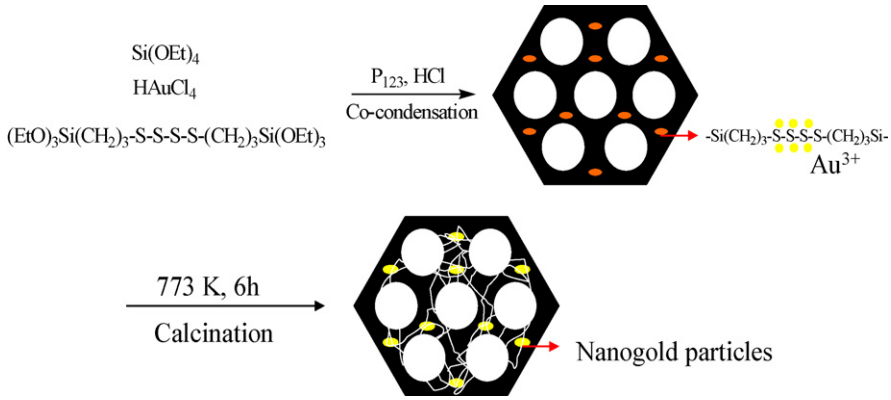


Scheme 1. Graphical representation of the preparation processes for mesoporous silica catalysts with gold nano-particles in the walls.

tetrasulfide, could be clearly observed for the typical as-synthesized 1.5% GMS. The FTIR spectrum of the 1.5% GMS also gave a narrow and intense band at 3740 $cm^{-1}$ and a broad low-frequency band centered at 3450 $cm^{-1}$. The band at 3740 $cm^{-1}$ can be assigned to the symmetrical stretching vibration mode of O–H from isolated terminal silanol (Si–OH) groups, while the broad low-frequency band at 3450 $cm^{-1}$ is due to those silanol groups or silanol ''nests'' with cross hydrogen-bonding interactions [19,20]. There was an abundance of silanol groups present in the as-synthesized 1.5% GMS. After calcination, the bands in the range of 2800–3000 $cm^{-1}$ disappeared completely, as well as an increase in intensity of the band at 3740 $cm^{-1}$ in the spectrum of Fig. 1b, demonstrating unambiguously the organic moieties had been removed from the catalyst surface for the GMS sample calcined at 773 K for 5 h. Thermogravimetric analysis results (Fig. 2) of the as-synthesized 1.5% GMS further demonstrate this point. Thermogravimetric analysis presented two weight decrease processes at 313 K (5 wt.%) and 623 K (32 wt.%), respectively. The former process was attributed to the desorption of physically adsorbed water species while the latter was due to the decomposition of the organic moieties. Similar results have been reported for organic group modified SBA-15, indicating the decomposition of organic composite in SBA-15 occurs at about 623 K [21,22].

Fig. 3 shows the typical nitrogen adsorption isotherm which is of Type IV for mesoporous silica. The adsorption isotherm showed a sharp inflection, which is a characteristic of capillary condensation within uniform mesopores. There was an uncommon hysteresis loop at $P/P_0$ values between 0.4 and 1 that might indicate that some structural defects were formed in the mesoporous framework [23,24]. Previous studies showed that MCM-41 or Al-MCM-41 with void defects can be synthesized using a ''delayed neutralization'' method in basic condition, the aluminum incorporation into the mesoporous framework and special morphologies always led to the formation of these structural defects [21,25]. In the GSM materials reported here, the formation of void defects might be attributed to the incorporation of gold in the walls of mesoporous silica. The surface area, pore volume and pore diameter obtained from $N_2$-adsorption measurements in Table 1 indicated that the surface area, pore volume and pore diameter decreased with the increasing of gold content. Normally, the BET surface area of pure SBA-15 is about 800 $m^2\ g^{-1}$ [26]. Numerous previous studies have indicated that the surface area and pore volume of mesoporous materials with metal nano-particles in the channels often are smaller than those of the corresponding pure mesoporous silica [27–30]. Under our preparation conditions, the BET surface area of pure SBA-15

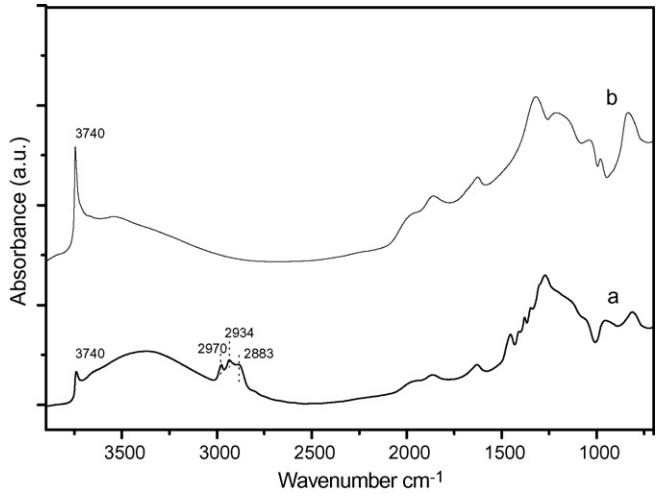


Fig. 1. FTIR spectra of 1.5% GMS before calcination (a) and after calcination (b).

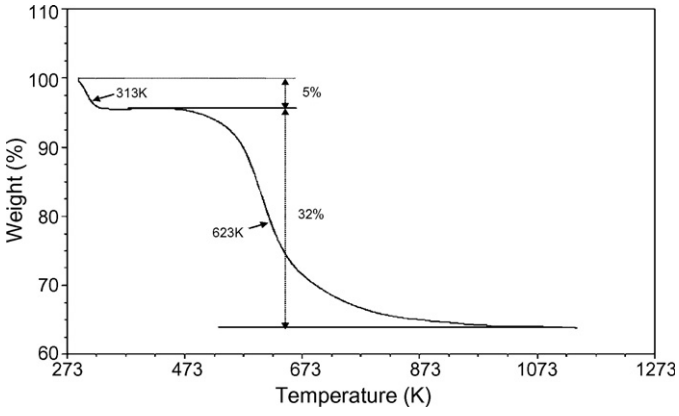


Fig. 2. Thermogravimetric analysis of the as-synthesized 1.5% GMS sample.

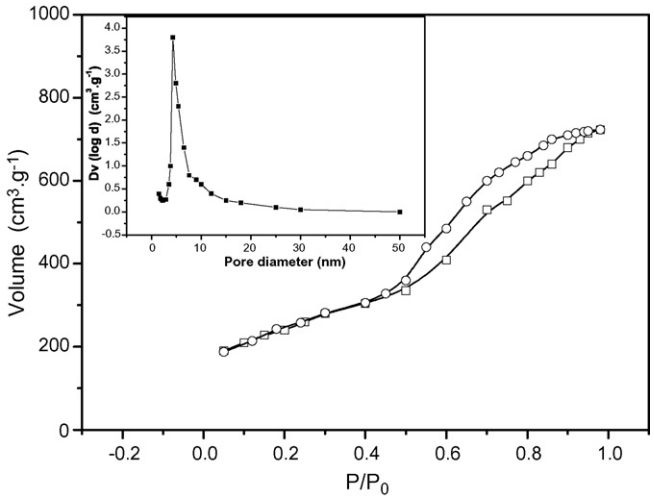


Fig. 3. Nitrogen adsorption–desorption isotherms and BJH pore size distribution plots (inset) of 2% GMS sample.

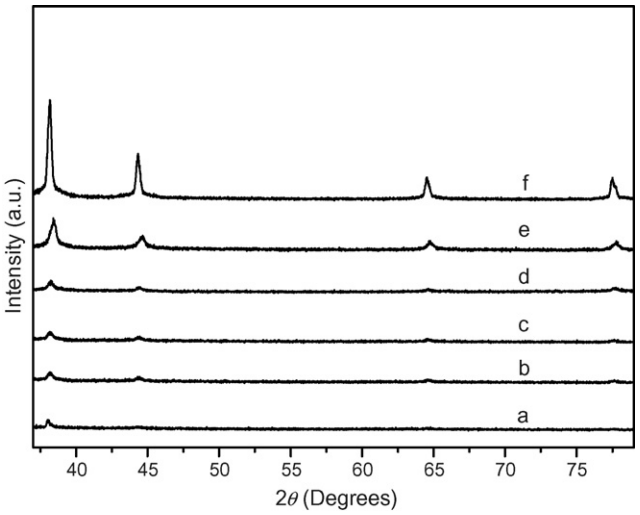


Fig. 4. XRD patterns of the catalysts: (a) 0.5% GMS, (b) 1.0% GMS, (c) 1.5% GMS, (d) 2.0% GMS, (e) 2.5% GMS and (f) 10% GMS.

was 788 $m^2\,g^{-1}$, pore volume was 1.1 $m^2\,g^{-1}$, and pore diameter was 6.2 nm. When the loading of gold was less than 2%, the surface area and pore volume were larger than that of pure SBA-15. The high surface area and pore volume may be attributed to the formation of void defects or micropores in the silica walls due to the introduction of gold nano-particles.

Fig. 4 shows the XRD patterns of these catalysts. The presence of characteristic diffraction lines at $2\theta = 38^\circ$, which are assigned to (1 1 1) planes of the face centered cubic structure of gold, indicated that the gold had crystallized. When the concentration of gold was less than 2%, the supported Au catalysts had very weak diffraction lines for gold, indicating that the gold concentrations were low in the mesoporous silica materials.

For the GMS catalysts, our initial studies focused on the oxidation of benzyl alcohol because this reaction is often employed as a model reaction for alcohol oxidation. Furthermore, this molecule was chosen because of its relatively high reactivity and because the main product is a non-enoliable aldehyde thus reducing the number of possible side products [10]. The reaction pathways of benzyl alcohol are not consistent in the previous literature. Some authors suggest that benzyl benzoate came from the aldol condensation following an oxidation [10]. On the other hand, in Ref. [14], it was suggested that benzyl alcohol is oxidized into benzaldehyde, then benzaldehyde is further oxidized into benzoic acid and finally benzyl alcohol and benzoic acid would interact and produce benzyl benzoate. In our case, the reactions involved in the oxidation process may be as follows:

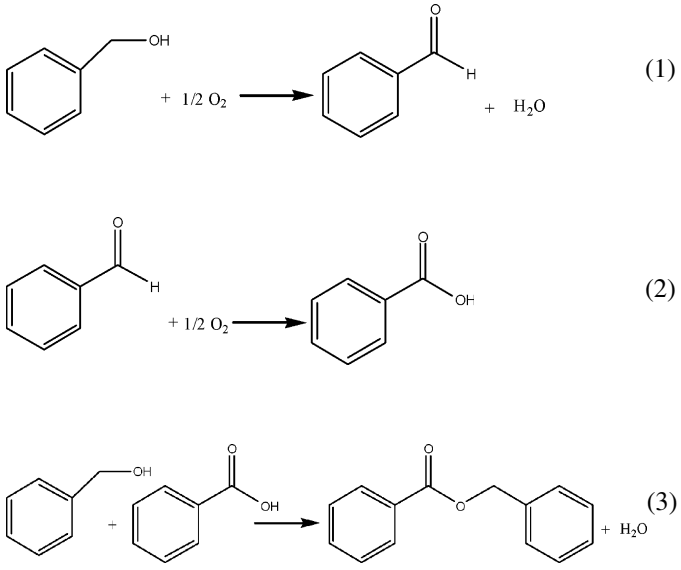


In the first step, benzyl alcohol is oxidized into benzaldehyde, then benzaldehyde is further oxidized into benzoic acid. In the presence of acid or base catalysts, benzyl alcohol and benzoic acid will interact and produce benzyl benzoate.

Table 1
$N_2$ adsorption/desorption parameters of pure SBA-15 and gold containing mesoporous catalysts

| Sample | Surface area BET ($m^2\,g^{-1}$) | Surface area BJH ($m^2\,g^{-1}$) | Pore volume ($cm^3\,g^{-1}$) | Pore diameter (nm) |
|---|---|---|---|---|
| Pure SBA-15 | 788 | 983 | 1.1 | 6.2 |
| 0.5% GMS | 1048 | 1376 | 1.6 | 4.9 |
| 1.0% GMS | 1067 | 1507 | 1.5 | 4.8 |
| 1.5% GMS | 822 | 1315 | 1.3 | 4.8 |
| 2.0% GMS | 818 | 1018 | 1.2 | 4.8 |
| 2.5% GMS | 759 | 909 | 1.0 | 4.8 |
| 10% GMS | 643 | 791 | 0.8 | 4.3 |

Table 2
Results of benzyl alcohol oxidation to benzyldehyde over mesoporous silica framework stabilized nanogold catalysts

| Catalyst | Conversion of benzyl alcohol (%) | Selectivity (%) | | | Yield of benzaldehyde (%) | TOF (mol mol$^{-1}$ (Au) h$^{-1}$)[a] |
|---|---|---|---|---|---|---|
| | | Benzaldehyde | Benzoic acid | Benzyl benzoate | | |
| 0.5% GMS | 6.4 | 100 | – | – | 6.4 | 280 |
| 1.0% GMS | 15.3 | 98.8 | – | 1.2 | 15.1 | 331 |
| 1.5% GMS | 26.2 | 98.3 | – | 1.7 | 25.8 | 377 |
| 2.0% GMS | 35.0 | 95.6 | 1.0 | 3.4 | 33.5 | 367 |
| 2.5% GMS | 42.8 | 94.9 | 1.2 | 3.9 | 40.6 | 356 |
| 10% GMS | 57.7 | 74.3 | 14.7 | 11.0 | 42.9 | 94 |
| 2.5% GMS[b] | 52.6 | 51.4 | 38.1 | 10.5 | 27.0 | 59 |

Reaction conditions: 3.0 g benzyl alcohol, 50 mg catalyst, 15 atm $O_2$, 403 K, 5 h.
[a] Rate of the formation of benzyldehyde per mol gold per hour.
[b] Reaction time: 20 h.

For the solvent-free oxidation of benzyl alcohol under an oxygen pressure of 1.5 atm, 3.0 g benzyl alcohol with 50 mg catalysts was charged into an autoclave, then was stirred and heated to 403 K for 5 h. The reaction was followed by GC analysis and the products were identified by GC–MS analysis and compared with the standard sample. These catalytic results were summarized in Table 2. When the amount of gold is less than 2.0% the by-product was exclusively benzyl benzoate. Benzoic acid was not detected by GC indicating that it reacted immediately with benzyl alcohol as it was formed. With the 0.5% GMS catalysts, a conversion of 6.4% was observed which corresponded to a TOF of 280, while the selectivity to benzaldehyde was 100%. Conversion increased with increased loadings of gold while the selectivity to benzaldehyde decreased slightly. The TOF decreased when the amount of gold was larger than 1.5%, indicating that not all the gold introduced was active. For the 2.5% GMS catalyst an extended reaction time of 20 h led to a conversion of 52.6% but the selectivity to benzaldehyde decreased to 51.4% and there were large amounts of benzoic acid formed (38.1%) which did not immediately react with the benzyl alcohol. In order to enhance our understanding of the catalytic properties of the GMS catalysts, oxidation of alcohols under atmospheric pressure oxygen flow was also studied. Because the 1.5% GMS showed the highest TOF value for the solvent-free oxidation of benzyl alcohol, it was chosen for the atmospheric pressure oxidation. All reactions were carried out at 10 mmol scale, the molar ratios of substrate/catalyst (gold) are 1:0.0014. The results are summarized in Table 3. The 1.5% GMS was very active for atmospheric pressure oxidation of alcohols and the conversion could reach 100% at 2 h for benzyl alcohol. The methyl substituted benzyl alcohol oxidation was attempted with the catalyst in toluene in the presence of $K_2CO_3$ using molecular oxygen. The conversion of 4-methyl benzyl alcohol was 95% with 87% selectivity to the corresponding aldehyde at 2 h. The oxidation of cyclohexanol was also studied and the conversion could reach 32% with 100% selectivity to cyclohexanone in 2 h. Recycling experiments were examined for the atmospheric pressure aerobic oxidation of benzyl alcohol. Thus, for the first run, the 1.5% GMS catalyst gave a >99% conversion of benzyl alcohol, after recovery, the catalyst was successfully subjected to two more runs from which it gave the same >99% conversion of benzyl alcohol only with slight changes in the selectivity and reaction time. Fig. 5 shows the XRD patterns of

Table 3
Aerobic oxidation of alcohol to the corresponding aldehydes/ketones catalyzed by 1.5% GMS[a]

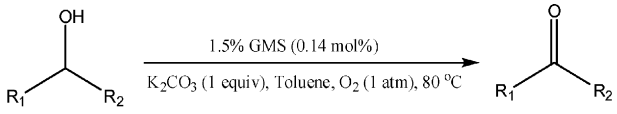


1 2

| Entry | $R_1$ | $R_2$ | Time (h) | Conversion of 1 (%) | Selectivity of 2 (%) | TOF (h$^{-1}$) | Yield of 2 (%) |
|---|---|---|---|---|---|---|---|
| 1 | Ph | H | 2.0 | >99 | 79 | 364 | 79 |
| 2[b] | Ph | H | 2.5 | >99 | 78 | 291 | 78 |
| 3[c] | Ph | H | 3.0 | >99 | 76 | 243 | 76 |
| 4 | 4-Me$C_6H_4$ | H | 2.0 | 95 | 87 | 346 | 83 |
| 5 | $-CH_2CH_2CH_2CH_2CH_2-$ | | 3.5 | 45 | 97 | 94 | 44 |
| 6 | $-CH_2CH_2CH_2CH_2CH_2-$ | | 2.0 | 32 | >99 | 116 | 32 |
| 7 | $-CH_2CH_2CH_2CH_2CH_2-$ | | 1.5 | 24 | >99 | 117 | 24 |

[a] All reactions were carried out at 10 mmol scale, the molar ratios of substrate/catalyst (gold) are 1:0.0014. The 10 mmol substrate, 0.14 mol% Au at SBA-15, 353 K, 1 atm $O_2$ (flow: 90 mL min$^{-1}$), 10 mmol $K_2CO_3$, 20 ml toluene. Conversion and selectivity were determined by GC using the starting alcohol as internal standards.
[b] The second use of the catalyst.
[c] The third use of the catalyst.

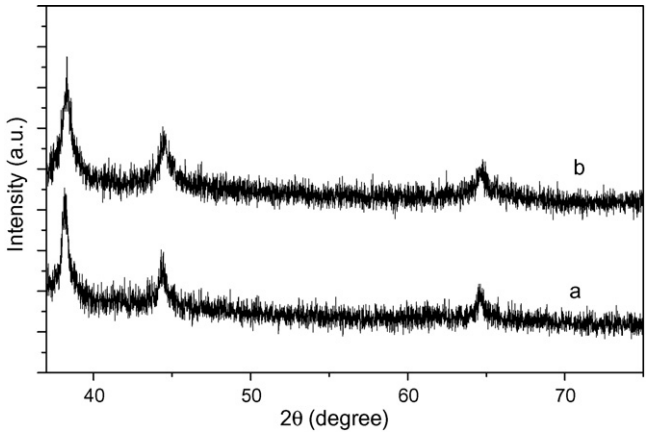


Fig. 5. XRD patterns of 1.5% GMS catalyst: (a) before reaction and (b) after the third catalytic run.

1.5% GMS catalyst before reaction and after the third catalytic run. The initial catalyst showed broad diffraction peaks of gold indicating small particles. The particle size (3.0 nm) was calculated from the full width at half maximum (FWHM) of Au (1 1 1) diffraction peak at the value of $2\theta = 38^{\circ}$ using the Scherrer equation. After the third catalytic run at 80 °C, the XRD pattern was nearly the same to that of the fresh catalyst clearly indicating that sintering of gold had not taken place.

The 1.5% GMS catalyzed atmospheric pressure aerobic oxidation of benzyl alcohol was also investigated by in situ DRIFT spectroscopy. Spectrum (a) in Fig. 6 was collected after the catalyst was exposed to the stream of flowing nitrogen carrying a small concentration of benzyl alcohol for 30 min. After the adsorbed benzyl alcohol catalyst was exposed to air flow for 30 min, cooled to room temperature and purged with nitrogen for 30 min to remove gas phase benzyl alcohol and benzaldehyde, spectrum (b) in Fig. 6 was collected. The characteristic peaks of benzyl alcohol in the region of 3100–3600 $cm^{-1}$ and benzaldehyde in the region of 1670–1720 $cm^{-1}$ were in good agreement with the previously reported results [31]. Gas-phase benzaldehyde often contains a very strong band at 1723 $cm^{-1}$ [32], as compared with free C=O groups, the stretching band of the C=O bond of adsorbed benzaldehyde showed a pronounced shift to lower wavenumbers (red shift). The red-shifted band at 1690 $cm^{-1}$ in Fig. 6(b) could be assigned to the stretching vibration of the C=O bond of adsorbed benzaldehyde. The result clearly indicated that benzaldehyde was formed after exposure to air. The weak and wide bands observed in Fig. 6(b) could be attributed to CO adsorption on the different sites of polycrystalline gold. The adsorbed CO might be formed by decarbonylation of benzaldehyde and might be the reason for the catalyst deactivation, similar results have been obtained on $Pd/Al_2O_3$ catalysts [33].

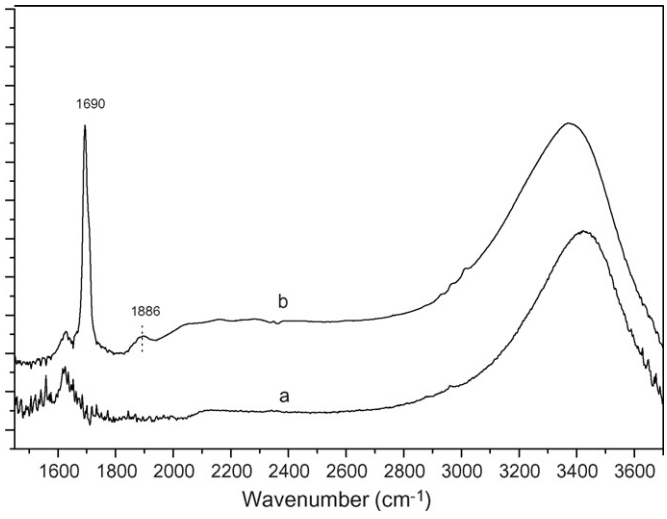


Fig. 6. In situ FTIR spectra of benzyl alcohol on 1.5% GMS catalyst: (a) in nitrogen and (b) after exposed to air and purged by nitrogen.

## 4. Conclusions

Mesoporous silica materials with nanoscale-gold in the framework were prepared by functionalizing the silica with thioether groups. Characterization of the materials demonstrated that they possess unusually high surface area and pore volume, the pore size distributions were very narrow, and there were large amounts of void defects in the pore walls. These materials were evaluated for the solvent-free liquid phase aerobic oxidation of benzyl alcohol by molecular oxygen. Benzaldehyde was obtained with high selectivity under the reaction conditions of 403 K, 15 atm and 5 h. The 1.5% GMS catalyst was also very active for atmospheric pressure aerobic oxidation of benzyl alcohol, was stable under the reaction conditions and the conversion was still better than 99% after recycling three times.

## Acknowledgement

The authors would like to thank the International University Bremen for financial support.

## References

[1] A. Dijksman, A. Marino-Gonzalez, A.M. Payeras, I.W.C.E. Arends, R.A. Sheldon, J. Am. Chem. Soc. 123 (2001) 6826.
[2] M. Hudlicky, Oxidations in Organic Chemistry, American Chemical Society, Washington, DC, 1990.
[3] R. Liu, X. Liang, C. Dong, X. Hu, J. Am. Chem. Soc. 126 (2004) 4112.
[4] T. Mallat, A. Baiker, Chem. Rev. 104 (2004) 3037.
[5] R.A. Sheldon, I.W.C.E. Arends, A. Dijksman, Catal. Today 57 (2000) 157.
[6] B.Z. Zhan, A. Thompson, Tetrahedron 60 (2004) 2917.
[7] B. Karimi, S. Abedi, J.H. Clark, V. Budarin, Angew. Chem. Int. Ed. 45 (2006) 4776.
[8] M. Haruta, Catal. Today 36 (1997) 153.
[9] M. Haruta, Stud. Surf. Sci. Catal. 110 (1997) 123.
[10] D.I. Enache, D.W. Knight, G.J. Hutchings, Catal. Lett. 103 (2005) 43.
[11] B. Guan, D. Xing, G. Cai, X. Wan, N. Yu, Z. Fang, L. Yang, Z. Shi, J. Am. Chem. Soc. 127 (2005) 18004.
[12] A. Abad, P. Concepcion, A. Corma, H. Garcia, Angew. Chem. Int. Ed. 44 (2005) 4066.
[13] D.I. Enache, J.K. Edwards, P. Landon, B. Solsona-Espriu, A.F. Carley, A.A. Herzing, M. Watanabe, C.J. Kiely, D.W. Knight, G.J. Hutchings, Science 311 (2006) 362.
[14] V.R. Choudhary, A. Dhar, P. Jana, R. Jha, B.S. Uphade, Green Chem. 7 (2005) 768.

[15] C.W. Corti, R.J. Holliday, D.T. Thompson, Appl. Catal. A 291 (2005) 253.
[16] J. Gu, J. Lin, G. You, L. Xiong, S. Qian, Z. Hua, H. Chen, Adv. Mater. 17 (2005) 557.
[17] K. Zhu, J. Hu, R. Richards, Catal. Lett. 100 (2005) 195.
[18] C. Yang, H. Sheu, K. Chao, Adv. Funct. Mater. 12 (2002) 143.
[19] Z. Luan, J.A. Fournier, J.B. Wooten, D.E. Miser, Micropor. Mesopor. Mater. 83 (2005) 150.
[20] S.-C. Shen, S. Kawi, J. Phys. Chem. B 103 (1999) 8870.
[21] X. Wang, K.S.K. Lin, J.C.C. Chan, S. Cheng, J. Phys. Chem. B 109 (2005) 1763.
[22] L. Li, J. Shi, J. Yan, X. Zhao, H. Chen, Appl. Catal. A 263 (2004) 213.
[23] H.P. Lin, S.T. Wong, C.Y. Mou, C.Y. Tang, J. Phys. Chem. B 104 (2000) 8967.
[24] J. Liu, J. Yang, Q. Yang, G. Wang, Y. Li, Adv. Mater. 15 (2005) 1297.
[25] H.P. Lin, Y.P. Cheng, C.Y. Mou, Chem. Mater. 10 (1998) 3772.
[26] D.Y. Zhao, J.L. Feng, Q.S. Huo, N. Melosh, G.H. Fredrickson, B.F. Chmelka, G.D. Stucky, Science 279 (1998) 548.
[27] C. Sener, T. Dogu, G. Dogu, Micropor. Mesopor. Mater. 94 (2006) 89.
[28] X. Xu, J. Li, Z. Hao, W. Zhao, C. Hu, Mater. Res. Bull. 41 (2006) 406.
[29] C. Aprile, A. Abad, H. Garcia, A. Corma, J. Mater. Chem. 15 (2005) 4408.
[30] C. Yang, P. Liu, Y. Ho, C. Chiu, K. Chao, Chem. Mater. 15 (2003) 275.
[31] R.J.J. Jachuck, D.K. Selvaraj, R.S. Varma, Green Chem. 8 (2006) 29.
[32] J. Lichtenberger, S.C. Hargrove-Leak, M.D. Amiridis, J. Catal. 238 (2006) 165.
[33] C. Keresszegi, D. Ferri, T. Mallat, A. Baiker, J. Phys. Chem. B 109 (2005) 958.